
Image Quality of the Human Eye

Susana Marcos, Ph.D.

■ Factors Contributing to Retinal Image Degradation

The eye is an optical instrument that projects scenes of the visual world onto the retina. It has been known for many years that the eye is far from being a perfect optical system, in particular for large pupil diameters. Refractive anomalies (defocus or astigmatism) occur frequently in the eye. In Western countries, myopia affects approximately 30% of the population, although its prevalence is much higher (> 80%) in certain Asian societies.¹ However, the eye suffers also from other optical imperfections (called high-order *aberrations*), which are not typically measured in the clinic and cannot be corrected by conventional means. Like defocus, optical aberrations blur the retinal image, reducing image contrast and limiting the range of spatial frequencies available to further stages of the visual processing. The contribution of aberrations to optical degradation is typically smaller than is that of defocus or astigmatism. The blurring effect of aberrations becomes more noticeable for large pupils. For small pupil sizes, diffraction effects, associated with limited aperture size, predominate over the aberrations.

Along with diffraction and aberrations, scattering also contributes to degradation of retinal image quality. Scattering occurs at the cornea² and particularly in the lens.³ Although typically scattering is small in normal, young eyes, it is well known that it increases with age (due to changes in the crystalline lens⁴) and after PRK refractive surgery.⁵

■ Functions Describing the Optical and Retinal Image Quality of the Human Eye

Optical systems are typically described by the modulation transfer function.^{6,7} The MTF represents the decrease in sinusoidal grating contrast as a function of spatial frequency. The human eye is a low-pass filter

(i.e., contrast losses increase with spatial frequency), and the MTF is generally different for different grating orientations. The contrast sensitivity function (CSF, the change of contrast perception as a function of spatial frequency) is the psychophysical equivalent to the MTF. The MTF accounts for the contrast degradation due only to the optics of the eye.

The point spread function (PSF) is also commonly used to describe the performance of optical systems.^{6,7} It represents the intensity distribution of a point source as imaged through the optical system. The PSF for diffraction-limited optical systems with a circular aperture is the airy disk. Optical aberrations and scattering produce further spread of the image of a point source. In the eye, small pupils (approximately 1 mm) produce diffraction-limited PSFs. For larger pupils, aberrations tend to be the dominant source of degradation.^{8,9} Figure 1 shows the PSF for three different pupil sizes for an aberration-free (diffraction-limited) system and for an eye with aberrations. The PSF and MTF are sometimes called *image quality functions*, since they represent the quality of the images rendered by the optical system. The most common image quality metric based in these functions is the strehl ratio. The strehl ratio represents the maximum of the PSF relative to the maximum of the diffraction-limited PSF for the

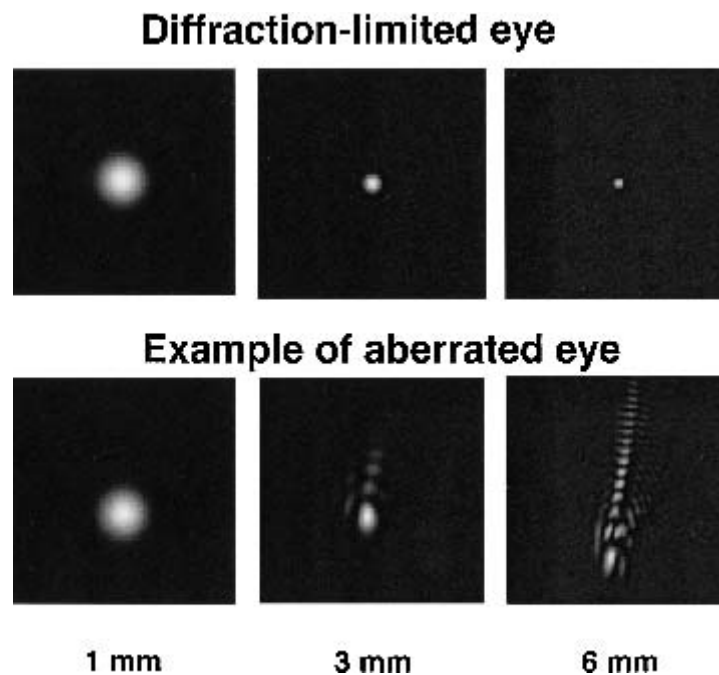


Figure 1. Point spread functions (i.e., the image of a point source on the retina), in a theoretically perfect eye (upper row) and in an eye with aberrations (lower row), for three different pupil diameters.

same pupil size, or equivalently the volume of the MTF relative to the volume under the diffraction-limited MTF for the same pupil size. A system is typically considered diffraction-limited if the strehl ratio is higher than 0.8 (Rayleigh criterium).

Optical designers often make use of geometrical optics to assess the optical quality of an imaging system by computing the optical path of a set of parallel rays entering the optical system. In a perfect optical system, rays entering through different parts of the pupil hit the image plane (the retina in the case of the eye) at the same location. Imperfections of the optics cause departure of those rays from the ideal location. These angular deviations are called *transverse aberrations*.^{6,10} The most common representation of the aberrations of the optical system is in terms of the wave aberration, which is defined as the departure of the wave aberration from its ideal wave form. The wavefront is normal to the trajectories of the rays. This wavefront is a spherical wave for the perfect optical system and a distorted wave for an aberrated system. The difference between the aberrated wavefront and the ideal spherical wavefront is called *wave aberration*. The wave aberration is measured at the pupil plane and is represented as a “topographical” map. For a perfect optical system, the wave aberration is flat across the pupil. A typical way to describe the wave aberration is in terms of a Zernike polynomial expansion.^{6,10–12} Zernike coefficients

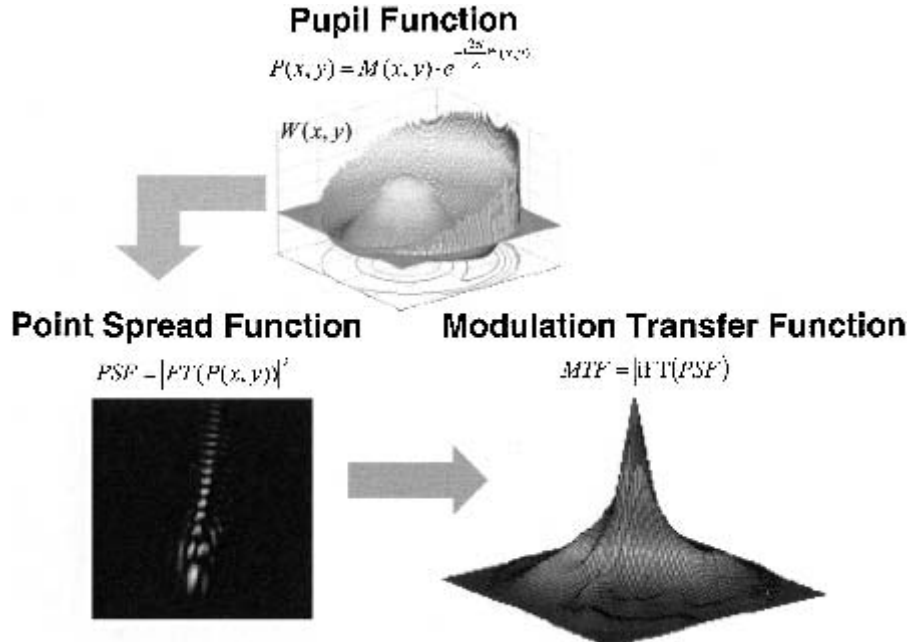


Figure 2. Mathematical relations between the wave aberration (as phase of the pupil function), modulation transfer function, and point spread function.

represent the weight of each simpler polynomial in the wave aberration. The low-order terms correspond to conventional refractive errors: first-order terms represent the prism, and second-order terms represent defocus and astigmatism. High-order terms include other well-known monochromatic aberrations (i.e., spherical aberration due to changes in focus with pupil size or coma, a third-order, nonrotationally symmetrical aberration). The root-mean-square (RMS) wavefront error can be estimated from the wave aberration, and it is used as a global optical quality metric. Mathematical computations allow direct estimation of the PSF and MTF from the wave aberration,⁷ as depicted in Figure 2. The phase of the pupil function is proportional to the wave aberration. The PSF is the squared modulus of the Fourier transform of the pupil function, and the MTF is the modulus of the inverse Fourier transform of the PSF. It should be noted that, unlike the MTF estimated from double-pass measurements, the MTF computed from the wave aberration does not contain the effects of scattering. However, while the MTF is easily obtained from the wave aberration (for any pupil size and, computationally, for every focus), the wave aberration or even the PSF cannot be estimated directly from the double-pass MTF estimates (unless complicated phase retrieval algorithms are applied¹³).

■ Measurement of Monochromatic Retinal Image Quality with the Double-Pass Technique

Vision scientists have measured the ocular MTF for years. Early estimates of the MTF were obtained by direct measurements of the CSF with sinusoidal fringes presented on a CRT monitor and measurements of the CSF using interference fringes projected directly on the retina, bypassing the ocular optics.^{14,15} The former includes the neural and the optical degradation, while the latter includes only the neural degradation. The MTF is then estimated as the ratio between conventional and the interferometrical CSF. This method provides accurate estimates of the MTF, validated through other techniques, but was very time-consuming, particularly if a wide range of spatial frequencies and grating orientation were tested.

The double-pass technique is an objective alternative for fast measurements of the retinal image quality and of the MTF in particular.¹⁶⁻²⁰

AV1.F3 Figure 3, upper row shows the basic principle of the double-pass system. In this technique, a laser point source is projected on the retina, and its reflection off the retina is captured on a CCD camera placed at a conjugate plane. The aerial image captured by the CCD is the autocorrelation of the PSF, and the MTF can be easily estimated from the aerial image. This MTF incorporates the degradation imposed by monochromatic aberrations, diffraction, and scattering.

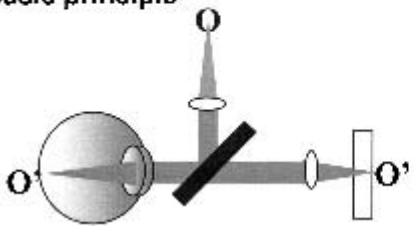

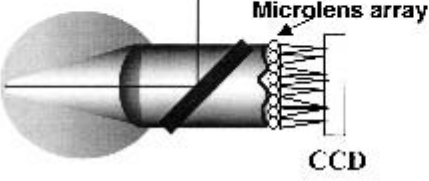
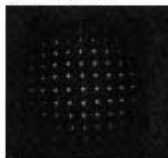
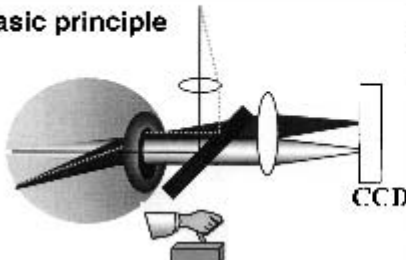
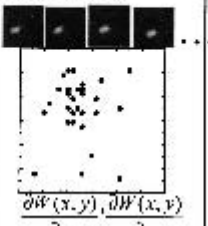
A. Double-pass technique		
Basic principle 	Raw data  Aerial image $O'' = PSF * PSF$	Result $MTF = \sqrt{O''}$
B. Outgoing aberrometry (i.e. SH)		
Basic principle 	Raw data  $\frac{\partial W(x, y)}{\partial x}, \frac{\partial W(x, y)}{\partial y}$	Result $W(x, y)$
C. Ingoing aberrometry (ie. LRT or SRR)		
Basic principle 	Raw data  $\frac{\partial W(x, y)}{\partial x}, \frac{\partial W(x, y)}{\partial y}$	Result $W(x, y)$

Figure 3. Basic concept of the double-pass technique and different aberrometers. (A) In the double-pass technique, a point source is projected onto the retina, and the image (after passing twice the ocular media) of the point is collected one CCD camera. This aerial image contains twice the degradation by the ocular optics, and it is the autocorrelation of the point spread function (PSF). The modulation transfer function (MTF) can be directly computed from the aerial image. (B) Principle of the Shack-Hartmann (SH) device. (C) Principle of two ingoing aberrometers (laser ray tracing [LRT] and spatially resolved refractometer [SRR]). In these two aberrometers, rays of light enter the eye through different parts of the pupil. By the effect of aberrations, eccentric beams are deviated with respect the principal ray. In LRT, the aerial images are captured onto a CCD camera, as a beam scans the pupil. In SRR, the subject aligns the beam with respect to a centered reference by means of a joystick. In both B and C, the raw data are the derivatives of the wave aberration.

■ Measurement of Monochromatic Retinal Image Quality with Aberrometers

Most current aberrometers measure the transverse aberration as a function of pupil position. The transverse aberrations are proportional to the local derivative (slope) of the wave aberration; therefore, the wave aberration can be easily retrieved from the transverse aberration. Transverse aberration can be measured as the test beam goes into the eye (ingoing aberrometry) or as the wavefront emerges from the eye (outgoing aberrometry). Figure 3 shows the basic principles of these two types of aberrometers. We describe briefly the aberrometers used in the experimental studies shown in the next sections: the Shack-Hartmann (S-H) wavefront sensor, which is an outgoing aberrometer, and two ingoing aberrometers, the laser ray tracing (LRT) and spatially resolved refractometer (SRR).

In the SH²¹⁻²³ (see Fig 3, middle panel), a narrow beam from a point light source is imaged by the eye onto the retina. The reflected wave travels through a lenslet array that focuses multiple spots (one per lenslet) onto a CCD camera. Each lenslet samples a small part of the wavefront corresponding to a certain pupil location. For a perfect optical system, the spots will be imaged at the focal point of each lenslet. The aberrations will cause local tilts of the wavefront; therefore, the spots will be deviated from the focal points. The transverse ray aberration associated with each lenslet can be determined from the departure of the centroid of its corresponding image with respect to the ideal position.

In the LRT²⁴⁻²⁶ (see Fig 3, lower panel), the pupil is sampled sequentially as a laser beam is scanned across the dilated pupil and projects a spot onto the retina. A CCD in a plane conjugate to the retina captures the aerial images as a function of entry pupil. By the effect of aberrations, rays entering the eye through eccentric locations are deviated from the central ray. The local transverse aberration is measured as the angular distance between the centroid of each of the aerial images and the centroid of the image corresponding to a centered entry pupil. Again, the wave aberration is estimated from the set of local transverse aberrations.

The SRR^{25,27-29} is also a sequential technique and also measures the aberrations in the first pass. The principle is similar to that of the LRT. Instead of capturing the image reflected by the retina onto a CCD camera, the subject aligns a cross-hair target viewed through a centered pupil with spots viewed through eccentric pupils.

These three techniques have been used extensively in the laboratory to understand the optical properties of the normal eye, as well as in clinical applications. For normal subjects, it has been demonstrated that the three techniques provide similar results. Most recent imaging system use infrared illumination, while for many applications, aberration data in visible light are required. It has been shown experimentally that, in gen-

eral, measurements in IR (780 nm) and in green light (543 nm) are equivalent³⁰, provided that the ocular longitudinal chromatic aberration (see next section) is taken into account. Also, the aberration data are unaffected by the state of polarization of the test beam.^{26,31}

The methods described measure the aberrations of the entire optical system of the eye. Conventional corneal topography can be used to measure the aberrations of the cornea alone.^{32–35} By performing virtual ray tracing on corneal elevation maps (obtained from placido disk corneal topography), the transverse aberration of the anterior corneal surface can be measured. From these data, the corneal wave aberration can be obtained, as described.

■ Polychromatic Retinal Image Quality

Both the double-pass and the aberrometry techniques described use monochromatic illumination and, therefore, measure monochromatic image quality. However, the visual world is polychromatic, and chromatic aberrations play an important role in image quality. The two major chromatic aberrations are the longitudinal chromatic aberration (LCA), the change of focus with wavelength, and the transverse chromatic aberration (TCA), the change of angular deviations with wavelength, and both are a major consequence of the wavelength dependence of the refractive index of the ocular media.³⁶ The LCA has been measured both through psychophysical techniques (see, for example, reviews by Charman³⁷ and Atchison and Smith³⁸) or using double-pass techniques at different wavelengths.^{39,40} Most reports in the literature show little LCA variation across individuals, although whether there are age-related changes seems to be controversial.^{41–43} We recently obtained LCA from aberration measurements (defocus term in the Zernike polynomial expansion) using the SRR at various wavelengths in the visible. Thibos and coworkers⁴⁴ proposed an equation, based on Cornu's expression for the dependence of the refractive index with wavelength, that fitted the experimental data. The average chromatic difference of focus between the blue (450 nm) and the red (650 nm) is 1.4 D. While the LCA of the human eye has been well studied, there are few reports for the TCA. Thibos and associates³⁶ and Simonet and Campbell⁴⁵ used a psychophysical vernier acuity technique to measure foveal transverse chromatic aberration. Typically, the TCA is not 0 at the pupil center. Foveal TCA reaches a minimum at a particular pupil position, known as *visual axis*. TCA is generally attributed to the fact that the eye is not a centered optical system (the fovea does not lie on the optical axis) and to pupil decentrations.^{36,46} Marcos and colleagues⁴⁷ used the SRR to measure TCA (angular deviations between blue and red test spots) and studied the influence of the aberrations and cone directionality on TCA. They concluded that TCA varied significantly across the population. However, this variability was not related to the variability in the

foveal location or pupil centration but rather may be associated with irregularities in the ocular components.⁴⁸

Measurements with the SRR at different wavelengths allowed estimations of high-order monochromatic aberrations with various wavelengths, as well as the chromatic aberrations.⁴⁷ These data were used to generate the polychromatic PSF and MTF. PSFs for each wavelength were computed (as described previously). The individual PSFs were added, with appropriate interpolation, and the shift was predicted by the TCA and was weighted by the spectral sensitivity curve. MTFs were computed from the [E4] PSF. As shown in Figure 4 for a single subject, the white-light MTF is significantly lower than the monochromatic MTF. It should be noted that a perfect optical system, subject to LCA and TCA, shows a relatively larger contrast degradation by the effect of chromatic aberrations than does an aberrated optical system. A similar approach was applied to the estimation of the MTF available for each cone class. McLellan and coworkers⁴⁹ showed that for a perfect optical eye, the MTF for S-cones is largely degraded by chromatic defocus, compared to the MTF for M- and L-cones. However, for real eyes, while the MTF for M- and L-cones is reduced as compared to the perfect optical system, the MTF for S-cones is not significantly reduced (with respect to the M- and L-MTF). This fact indicates a certain degree of balance of optical (monochromatic and polychromatic) aberrations in the eye.

■ Role of the Pupil in Retinal Image Quality

Pupil size determines the relative contribution of diffraction and aberrations to image quality. For small pupils, optical quality is dominated by

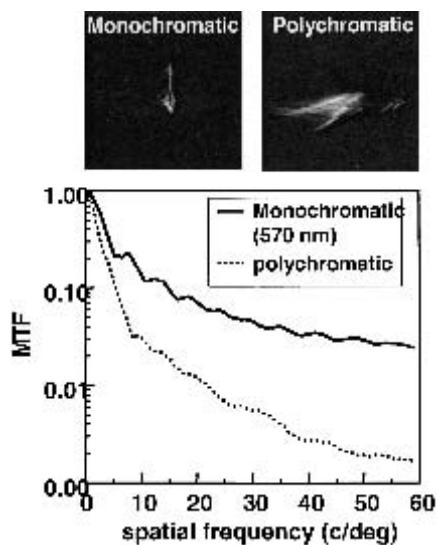


Figure 4. Monochromatic and polychromatic point spread functions (PSFs) for a normal, middle-aged patient and the corresponding modulation-transfer functions (MTFs) (radial profiles). Wave aberrations were measured at different wavelengths (450–650 nm) using the spatially resolved refractometer technique. Longitudinal chromatic aberrations (LCA) and transverse chromatic aberration (TCA) were obtained from the same set of data. PSFs and MTFs were computed as indicated in Figure 2. Polychromatic PSFs were generated by superposition of monochromatic PSF, weighted by the retinal spectral sensitivity. Best focus was set at 570 nm, the rest of wavelengths being defocused according to the LCA. Each monochromatic PSF was shifted to account for the effect of the TCA. All data are for 6-mm pupils. (Plot adapted from Marcos et al.⁴⁷)

diffraction, and aberrations have little effect, but the spatial resolution is low. For aberrated eyes and dilated pupils, the effect of diffraction is small as compared to the contribution of optical aberrations. See Figure 1 to see the differences in the PSF for a perfect system (only limited by diffraction) and a real eye with aberrations. The optimal pupil diameter (i.e., providing best resolution) depends on the actual amount and distribution of aberrations as well as on the wavelength but, in a typical eye, is around 3 mm.⁸ If there were no aberrations (or they could be corrected), the highest resolution would be achieved for the largest pupil diameter.

Double-pass MTF or ocular wave aberration measurements can be made with respect to different reference axes. Possible axes include the foveal achromatic axis (also known as *visual axis*), the keratometric axis, or the line of sight. The estimated aberrations will depend on the reference axis, and the computed MTF or PSF will also be different, depending on where the entrance pupil is centered.^{50,51} Double-pass measurements showed a sharp decline in image quality when a small artificial pupil was moved from the center to the edge of the natural pupil.⁵⁰ The Optical Society of America Standards Committee recommended the use of the line of sight (axis joining the fovea with the natural pupil center) as the reference axis for aberration measurements in the eye.⁵²

The depth of field of the eye is partly determined by the pupil size. However, while for the diffraction-limited optical system the depth of field decreases systematically with increasing pupil diameters, the presence of aberrations tends to equalize the depth of field to approximately 0.3 D (using the maximum intensity of the double-pass aerial image as the retinal image quality metric) beyond 4 mm.⁵³

Although it is generally assumed that the effective pupil is the natural (circular) pupil of the eye, this is not strictly true. Light efficiency is not uniform across the pupil, as a consequence of the directional properties of the photoreceptors (which absorb light more efficiently when they are illuminated along their axes). This effect is known as the *Stiles-Crawford effect*,⁵⁴⁻⁵⁶ which results in a gaussian effective pupil. The Stiles-Crawford effect was typically measured through psychophysical techniques, although much faster, reflectometric techniques have been developed recently.⁵⁷⁻⁶⁰ The peak of the Stiles-Crawford function is not necessarily the pupil center, since cones are pointing toward eccentric pupil locations in a significant amount of subjects.^{61,62} The SC peak is typically mirror-symmetrical between right and left eyes of the same individual. In general, the Stiles-Crawford effect diminishes the impact of aberrations (and therefore improves image quality), particularly for large pupils.^{63,64} Figure 5 shows computations of the MTF for one subject, without (constant pupil transmission) and with (gaussian pupil transmission) the Stiles-Crawford effect. It should be noted that for this particular subject, the Stiles-Crawford peak was -1.62 mm inferior and $+0.23$ mm temporal. Atchison and associates⁶⁵ showed that visual acuity decreased when the Stiles-

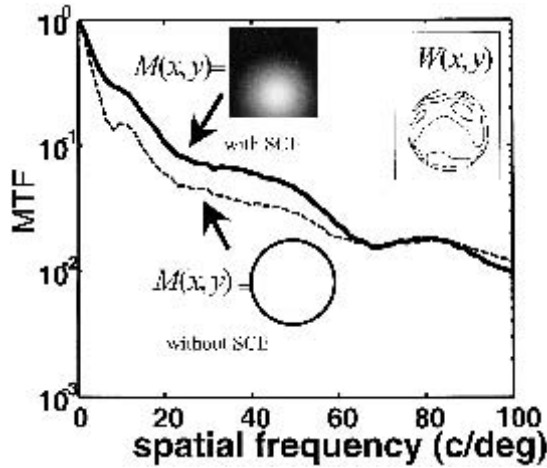


Figure 5. Modulation transfer function (radial profile) for one normal eye with and without taking into account the Stiles-Crawford effect (SCE). If the SCE is ignored, the modulus of the pupil function ($M(x,y)$) is 1 across the pupil. The SCE results in a gaussian luminous efficiency. The reflectometric SCE was measured for this patient using the technique from Burns et al.⁵⁷ All the computations were made for a 6-mm pupil. The wave aberration for this patient is shown in the inset (contour lines every $0.5 \mu\text{m}$). (Wave aberration and cone directionality data from Marcos and Burns.⁶¹)

Crawford effect was cancelled with special filters and increased when the effect was artificially doubled, particularly for out-of-focus conditions. Also, when the Stiles-Crawford peak was artificially moved, visual acuity changed (typically decreased for symmetrical pupil locations from the real peak.)⁶⁶

Retinal Image Quality in the Normal Human Eye

Variation Across Individuals Retinal image quality varies greatly among the population. Several population studies show a wide distribution of the aberrations in human eyes,^{67–69} typically all high-order terms averaging to 0, except for the spherical aberration that tends to be slightly positive. This variation in high-order aberrations parallels well-known variation in refractive errors. Figure 6 shows examples of the wave aberrations and the corresponding PSFs (computed as indicated in Fig 2) of a group of normal, young patients. Aberrations tend to be mirror-symmetrical between left and right eyes,⁶⁸ although similarly to those with anisometropia, patients with very different left-to-right wave aberration patterns are not uncommon.⁶¹

Sources of Aberrations in the Eye The cornea and the crystalline lens are the major refractive components in the eye, and aberrations of the individual components are expected to contribute to overall image quality. It has been shown that at least for young eyes, a proportion of the corneal aberrations are compensated by aberrations of the crystalline lens. A partial compensation of corneal astigmatism by the crystalline lens was well known in the clinical optometry literature (Java's rule).⁷⁰ Also, the fact that the spherical aberration of the cornea is typically positive, while the spherical aberration of the crystalline lens tends to be negative, has

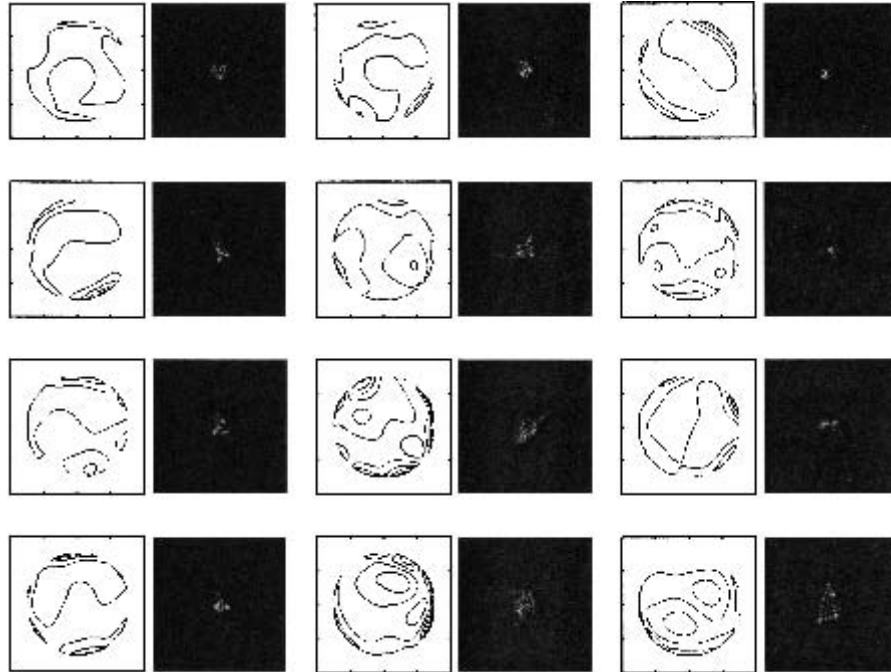


Figure 6. Examples of wave aberrations and corresponding point spread functions for a group of normal young patients (aged 23–29; spherical error, from -2.5 to -8 D). Pupil diameter, 6.5 mm. Contour line spacing; $0.5 \mu\text{m}$. (Wave aberration data from Marcos et al.¹⁰⁰)

been known for several years.⁷¹ Interestingly, a partial compensation of asymmetrical aberrations, such as coma, also seems to occur, at least in young, low myopic eyes.⁷² Several models have been attempted to explain the interactions of corneal and internal aberrations. However, simple tilts and decentrations of the ocular components are not sufficient to explain the complex structure of the total wave aberration pattern.

Changes with Accommodation The fact that the retinal image quality changes with accommodation has been shown in double-pass⁷³ or aberrometry studies.^{74,75} He and coworkers⁷⁵ reported aberration measures in a group of eyes for accommodation stimuli ranging from 0 D (infinity) to 6 D, using the SRR. As reported earlier in the literature, the lag of accommodation increases with accommodation demand.⁷⁶ As shown in [Figure 7A](#), optimal optical quality (excluding defocus and astigmatism) was attained for approximately 2 D, while the RMS increased by approximately $1 \mu\text{m}$ on average for 6 D of accommodation. The most systematic changes were found for the spherical aberration term (decreasing in all subjects and going from positive to negative in several subjects) and the higher-order aberrations. These changes are likely related to changes in

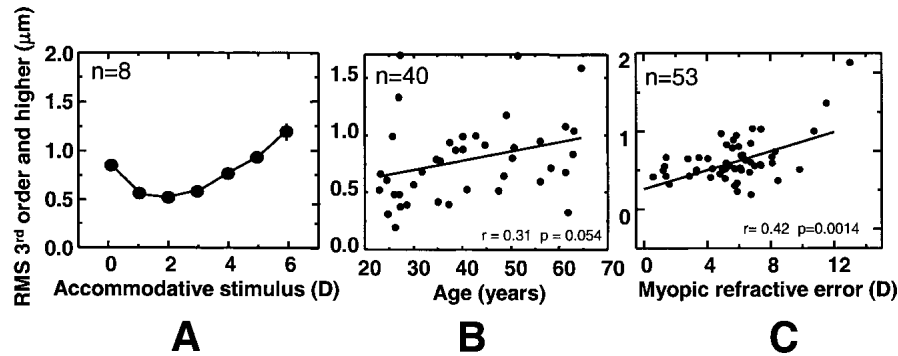


Figure 7. Root-mean-square (RMS) wavefront error for third- and higher-order aberrations. (A) As a function of accommodation (Data from He *et al.*⁷⁵). (B) As a function of age (Data from McLellan *et al.*⁸³). (C) As a function of refractive error (Data from Marcos *et al.*⁹²).

the shape of the crystalline lens during the accommodation process.^{77,78} Hofer and colleagues⁷⁹ measured dynamic changes of high-order aberrations during the accommodation process (0–2 D), and found temporal changes even when the accommodation was paralyzed by topical drugs.

Changes with Age Double pass MTFs show a decline of contrast transfer at all spatial frequencies between young and old patient. Part of the degradation is likely due to an increase of intraocular scattering with age.⁸¹ However, aberration measurements have revealed that part of the decrease in retinal image quality with age is due to an increase in ocular aberrations.^{82,83} McLellan and associates⁸³ showed (in a group of 38 patients ranging in age from 23 to 65 years) that third- and higher-order aberrations increase with age (0.7–1 μm, for a 7.3-mm pupil, on average). Results from this study are shown in Figure 6B. While no significant changes were found for third-order terms, the correlation of spherical aberration and fifth- and higher-order terms with age was highly statistically significant. Measuring corneal and total aberrations in a group of 17 patients (aged 20–70 years), Artal and colleagues⁷² showed that part of the increase of optical aberrations with age was due to disruption of the compensation of corneal and internal aberrations, which was common in young patients.⁸⁴ This is not surprising for spherical aberration, since *ex vivo* measurements have shown that the spherical aberration of the crystalline lens shifted toward positive values with age.⁸⁵ The reasons why this also happens for asymmetrical terms is still to be understood.

Changes with Eccentricity Monochromatic image quality as a function of the visual angle has also been studied both through double-pass techniques^{86,87} and aberrometry.^{88,89} Double-pass studies showed a decline in retinal image quality with eccentricity.⁸⁷ The largest degradation was found for visual angles beyond 20 degrees. In the central 20-degree

field, Strehl ratio drops only from approximately 0.14 to 0.9 (average of 4 patients), suggesting that the eye follows a wide-angle lens design (non-optimal quality on axis—on the line of sight—but constant image quality over a wide visual field). Astigmatism and coma increase with retinal eccentricity. Once peripheral and astigmatic defocus are corrected, higher-order aberrations do not increase dramatically off axis. Navarro and coworkers⁸⁹ reported average increases in third and higher-order RMS (for a 6.5-mm pupil) from 0.45 μm at the fovea to 1.1 μm at 40 degrees.

Relationship with Refractive Error Several cross-sectional studies have measured high-order aberrations as a function of myopic refractive error, all showing a tendency of poorer optical quality in the higher myopes.⁹⁰ Marcos and colleagues^{91,92} reported results on 53 eyes (see Fig. 6C), showing a statistically significant increase of third- and higher-order RMS with myopia (from 0.3 μm for -0.25 D to 1 μm for 12 D, on average, for a 6.5-mm pupil). Corneal and internal aberrations also increased with myopia but at lower rates. Total spherical aberration did not change significantly with myopia. Corneal spherical aberrations increased toward more positive values for increasing myopia (associated with an increase in corneal asphericity) but tended to be compensated by the internal spherical aberration, which increased toward more negative values for increasing myopia. The major causes of increasing optical degradation with myopia were increased coma and higher-order aberrations.

Retinal Image Quality in the Pathological and Surgical Eye

The previous sections refer to retinal image quality in normal eyes. The techniques to measure retinal image quality and aberrations described have been applied clinically. They have proved to be valuable diagnostic and evaluation tools.

Optical Aberrations in Keratoconus Progressive distortion of the cornea in keratoconus leads to abnormal corneal topography and decreased visual performance in keratoconus patients. At least in early and moderate stages of the disease, most changes occur on the anterior corneal surface (i.e., the total aberration pattern is practically identical to the corneal aberration pattern; further changes in the posterior corneal surface may occur in the most advanced stages).⁹³ Astigmatism is typically high in these patients. Additionally, coma (normally in the vertical direction) is much higher than in normal patients^{33,94} (3.7 times on average, in a study by Barbero and coworkers.³³

Change of Optical Aberrations After Refractive Surgery Corneal refractive surgery has become a popular alternative for correction of re-

fractive errors. Early studies based on corneal topography showed that while defocus or astigmatism is generally successfully corrected, refractive surgery (RK, PRK and LASIK) increased the amount of corneal aberrations.^{95,96} In addition, the distribution of aberrations changed from the third-order dominance found in normal patients to fourth-order dominance. This increase in corneal aberrations correlates well with the decrease found in contrast sensitivity.³⁴ Seiler and coworkers,⁹⁷ in standard myopic PRK (15 eyes; mean preoperative spherical error, 4.8 D), and Moreno-Barriuso and associates,⁹⁸ for LASIK (22 eyes; mean preoperative spherical error, 6.5 D), measured for the first time the changes in the total aberration pattern induced by surgery. Both studies found a significant increase in third- and higher-order aberrations (by factors of 4.2 and 1.9 in the RMS, respectively). The larger increase occurred for spherical and third-order aberrations. Total, corneal, and internal (average across 14 eyes before and after surgery) from a study by Marcos and colleagues⁹⁸ are shown in Fig 7A). Marcos and coworkers⁹⁹ found that the decrease in the MTF computed from wave aberrations agreed with the decrease in contrast sensitivity measured psychophysically in those subjects. The changes of total spherical aberrations are not fully accounted by changes in the anterior corneal surface.¹⁰⁰ In all eyes, total spherical aberration increased slightly less than did corneal aberrations, likely due to significant changes in the posterior corneal shape (shifting toward more negative values of spherical aberration). The increase in the total spherical aberration is highly correlated to the amount of spherical error corrected, and it is associated with an increase in corneal asphericity. However, the causes of the increased asphericity are still not well understood.¹⁰¹ Refinement of ablation algorithms and a better understanding of the corneal biomechanical changes are needed to avoid induction of high-order aberrations.

Retinal Image Quality and Cataract Surgery In virtually all cataract procedures, the natural crystalline lens is replaced by artificial intraocular lenses (IOLs). IOL manufacturers typically assess the optical quality of these lenses by measuring the MTF and the resolution *in vitro*.¹⁰² The first measurements of the optical quality of patients with implanted IOLs were done using a double-pass technique.^{103,104} Postsurgical MTFs were lower than the MTFs of young eyes, and optical performance was worse with multifocal than with monofocal lenses. Recently, the aberrations of the IOL have been measured for the first time *in vivo*.¹⁰⁵ Corneal and total aberrations were measured using a videokeratoscope and LRT, respectively. The aberrations of the IOL were estimated as the total minus corneal aberrations. Figure 8B shows total, corneal, and internal aberrations in patients before and after cataract surgery (from a study by Barbero and colleagues¹⁰⁵). While scattering is removed with the extraction of the cataract and replacement by an IOL, aberrations are not reduced.

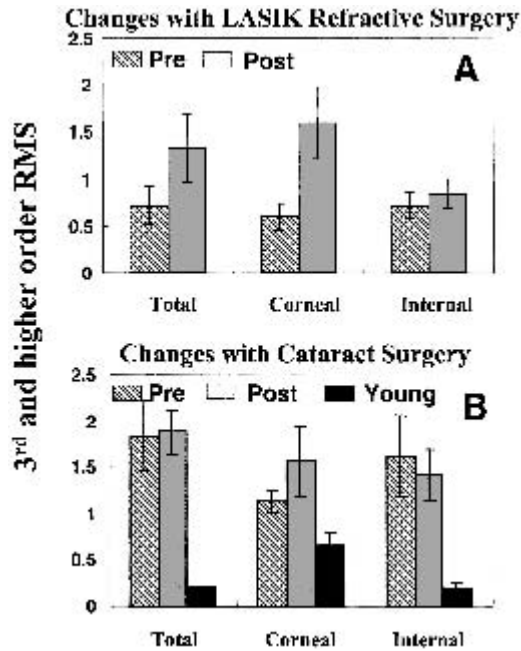


Figure 8. Root-mean-square (RMS) wavefront error for third- and higher-order aberrations for corneal, total, and internal aberrations. (A) In the same group of patients ($n = 14$) before and after LASIK refractive surgery for myopia, for a 6.5-mm pupil (From Marcos et al.¹⁰⁰) (B) In a group of patients before cataract surgery ($n = 6$), after cataract surgery by phacomulsification and acrylic IOL implant ($n = 9$), and a group of young emmetropic eyes ($n = 14$) (From Barbero et al.¹⁰⁵)

Corneal aberrations tend to increase with surgery, probably due to the incision. Pre- and post-cataract surgery aberrations are significantly larger than in a young control group. Measurements in vitro showed that the IOL is not aberration-free. The amount of aberrations (particularly astigmatism and third-order) increase after implantation, likely due to tilt and decentration of the lens. Similarly to what Artal and coworkers⁷² reported for old eyes, postsurgical eyes do not show a good balance of corneal and internal (IOL) aberrations. This is particularly due to the fact that the spherical aberration of the IOL tends to be positive. Further improvements of the surgical procedures and a lens design aiming at canceling the spherical aberration of the cornea may result in better optical outcomes of cataract surgery.

This study was supported by grant CAM 08.7/0010./2000 from Comunidad Autonoma de Madrid.

■ References

1. Grosvenor T, Goss DA. *Clinical management of myopia*. London: Butterworth-Heinemann, 1999
2. Hart RW, Farrell RA. Light scattering in the cornea. *J Opt Soc Am A* 1968;59:766–775

3. van den Berg T, Spekreijse H. Light scattering model for donor lenses as a function of depth. *Vision Res* 1999;38:1437–1445
4. Siew E, Opalecky D, Bettelheim F. Light scattering of normal human lens: II. Age dependence of the light scattering parameters. *Exp Eye Res* 1981;33:603–614
5. Merayo-Llodes J, Yañez B, Mayo A, et al. Experimental model of corneal haze. *J Refract Surg* 2001;17:696–699
6. Born M, Wolf E. *Principles of optics*, ed 6. Oxford: Pergamon Press, 1993
7. Goodman JW. *Introduction to Fourier optics*, ed 2. New York: McGraw-Hill International Editions, 1996
8. Artal P, Navarro R. Monochromatic modulation transfer function of the human eye for different pupil diameters: an analytical expression. *J Opt Soc Am A* 1994;11(1):246–249
9. Walsh G, Charman WN. The effect of pupil centration and diameter on ocular performance. *Vision Res* 1988;28:659–665
10. Malacara D. *Optical shop testing*, ed. 2. New York: John Wiley & Sons, Inc, 1992
11. Mahajan VN. Zernike circle polynomials and optical aberrations of systems with circular pupil. *Appl Optics* 1994;33:8121–8124
12. Thibos LN, Applegate RA, Schwiegerling JT, et al. Standards for reporting the optical aberrations of eyes. *Vision Science and its Applications, OSA Trends in Optics & Photonics* 2000;35:110–130
- AU2 13. Iglesias I, Berrio E, Artal P. Estimates of the ocular wave aberration from pairs of double-pass retinal images. *J Opt Soc Am A* 1998;15:2466–2476
14. Williams DR, Brainard DH, McMahon MJ, Navarro R. Double-pass and interferometric measures of the optical quality of the eye. *J Opt Soc Am A* 1994;11(12):3123–3135
15. Campbell FW, Green DG. Optical and retinal factors affecting visual resolution. *J Physiol (Lond)* 1965;181:576–593
16. Berny F. Etude de la formation des images rétinienne et détermination de l'aberration de sphéricité de l'oeil humain. *Vision Res* 1969;9:977–990
17. Westheimer G, Campbell FW. Light distribution in the image formed by the living human eye. *J Opt Soc Am* 1962;52:1040–1044
18. Charman WN, Jennings JAM. The optical quality of the monochromatic retinal image as a function of focus. *Br J Physiol Opt* 1976;31:119–134
19. Santamaría J, Artal P, Bescós J. Determination of the point-spread function of human eyes using a hybrid optical-digital method. *J Opt Soc Am A* 1987;4:1109–1114
20. Artal P, Marcos S, Navarro R, Williams DR. Odd aberrations and double pass measurements of retinal image quality. *J Opt Soc Am A* 1995;12:195–201
21. Liang J, Grimm B, Goetz S, Bille JF. Objective measurement of wave aberrations of the human eye with the use of a Hartmann-Shack wave-front sensor. *J Opt Soc Am A* 1994;11:1949–1957
22. Thibos LN, Faao P, Xin Hong M. Clinical applications of the Shack-Hartmann aberrometer. *Optom Vis Sci* 1999;76:817–825
23. Liang J, Williams DR. Aberrations and retinal image quality of the normal human eye. *J Opt Soc Am A* 1997;14:2873–2883
24. Navarro R, Losada MA. Aberrations and relative efficiency of light pencils in the living human eye. *Optom Vis Sci* 1997;74:540–547
25. Moreno-Barriuso E, Marcos S, Navarro R, Burns SA. Comparing laser ray tracing, spatially resolved refractometer and Hartmann-Shack sensor to measure the ocular wavefront aberration. *Optom Vis Sci* 2001;78:152–156
- AU3 26. Marcos S, Díaz-Santana L, Llorente L. Ocular aberrations with ray tracing and Shack-Hartmann wavefront sensors: Does polarization play a role? *J Opt Soc Am A* (in press) 2002
27. Webb RH, Penney CM, Thompson KP. Measurement of ocular wavefront distortion with a spatially resolved refractometer. *Appl Optics* 1992;31:3678–3686

28. He JC, Marcos S, Webb RH, Burns SA. Measurement of the wave-front aberration of the eye by a fast psychophysical procedure. *J Opt Soc Am A* 1998;15:2449–2456
29. Burns SA, Marcos S. Measurement of the image quality of the eye with the spatially resolved refractometer. In: MacRea S, Krueger R, Applegate R, eds. *Customized corneal ablations*. Thorofare, NJ: Slack (in press) 2000
- AU3** 30. Llorente L, Marcos S, Barbero S, et al. Ocular aberrations in infrared and visible light using a laser ray tracing technique. *Invest Ophthalmol Vis Sci* 2001(suppl):42:87
31. Prieto P, Vargas-Martín F, McLellan J, Burns S. The effect of the polarization on ocular wave aberration measurements. *J Opt Soc Am A* (in press) 2001
- AU3** 32. Barbero S, Marcos S, Merayo-Llodes JM. Exploring total and corneal aberrations in an unilateral aphakic subject. *J Cataract Refract Surg* (in press) 2002
- AU3** 33. Barbero S, Marcos S, Merayo-Llodes J, Moreno-Barriuso E. Validation of the estimation of corneal aberrations from videokeratography in keratoconus. *J Refract Surg* 2002; 18:263–270
- ED1** 34. Applegate R, Hilmante IG, Howland H, et al. Corneal first surface optical aberrations and visual performance. *J Refract Surg* 2000;16(5):507–514
35. Guirao A, Artal P. Corneal wave aberration from videokeratography: accuracy and limitations of the procedure. *J Opt Soc Am A* 2000;17:955–965
36. Thibos LN, Bradley A, Still DL, et al. Theory and measurement of ocular chromatic aberration. *Vision Res* 1990;30:33–49
37. Charman WN. The optics of the eye. In: Bass M, ed. *Handbook of optics*, ed 2. New York: McGraw-Hill, 1995
38. Atchinson DA, Smith G. *Optics of the human eye*. Oxford: Butterworth-Heinemann, 2000
39. Charman WN, Jennings JAM. Objective measurements of the longitudinal chromatic aberration of the human eye. *Vision Res* 1976;16:999–1005
40. Rynders MC, Navarro R, Losada MA. Objective measurement of the off-axis longitudinal chromatic aberration in the human eye. *Vision Res* 1998;38:513–522
41. Millodot M. The influence of age on the chromatic aberration of the eye. *Graefes Arch Klin Exp Ophthalmol* 1976;198:235–243
42. Mordt J, Adrian W. Influence of age on chromatic aberration of the human eye. *Am J Optom Physiol Opt* 1985;62:864–869
43. Howarth PA, Zhang XX, Bradley A, et al. Does the chromatic aberration of the eye vary with age? *J Opt Soc Am A* 1988;5:2087–2092
44. Thibos LN, Ye M, Zhang XX, Bradley AB. The chromatic eye: a new reduced-eye model of ocular chromatic aberration in humans. *Appl Optics* 1992;31:3594–3600
45. Simonet P, Campbell MCW. The optical transverse chromatic aberration on the fovea of the human eye. *Vision Res* 1990;30(2):187–206
46. Rynders MC, Lidkea BA, Chisholm WJ, et al. Distribution of pupil centers with respect to the visual axis. *Optom Vis Sci* 1993;70:157–158
47. Marcos S, Burns SA, Moreno-Barriuso E, Navarro R. A new approach to the study of ocular chromatic aberrations. *Vision Res* 1999;39:4309–4323
48. Marcos S, Burns SA, Prieto PM, et al. Investigating sources of variability of monochromatic and transverse chromatic aberrations across eyes. *Vision Res* 2001;41:3861–3871
49. McLellan JS, Marcos S, Prieto PM, Burns SA. Imperfect optics may be the eye's defense against chromatic blur. *Nature* (en prensa) 2002
- AU3** 50. Artal P, Marcos S, Iglesias I, Green DG. Optical modulation transfer function and contrast sensitivity with decentered small pupils. *Vision Res* 1996;6:3575–3586
51. Green DG. Visual resolution when light enters the eye through different parts of the pupil. *J Physiol* 1967;190:583–593
52. Applegate R, Thibos L, Bradley A, et al. Reference axis selection: subcommittee report of the OSA working group to establish standards for measurement and reporting of optical aberrations of the eye. *J Refract Surg* 2000;16:656–658

53. Marcos S, Moreno E, Navarro R. The depth-of-field of the human eye from objective and subjective measurements. *Vision Res* 1999;39:2039–2049
54. Stiles WS, Crawford BH. The luminous efficiency of rays entering the eye pupil at different points. *Proc R Soc Lond B Biol Sci* 1933;112:428–450
55. Enoch JM, Bedell HE. The Stiles-Crawford effects. Springer Series in Optical Sciences 1981
- AU4 56. Applegate RA, Lakshminarayanan V. Parametric representation of Stiles-Crawford functions: normal variation of peak location and directionality. *J Opt Soc Am A* 1993;10(7):1611–1623
57. Burns SA, Wu S, Delori F, Elsner AE. Direct measurement of human-cone-photoreceptor alignment. *J Opt Soc Am A* 1995;12(10):2329–2338
58. Delint PJ, Berendschot TTJM, Norren D. Local photoreceptor alignment measured with a scanning laser ophthalmoscope. *Vision Res* 1997;37(2):243–248
59. Gorrard JM, Delori FC. A reflectometric technique for assessing photoreceptor alignment. *Vision Res* 1995;35:999–1010
60. Marcos S, Burns SA. Cone spacing and waveguide properties from cone directionality measurements. *J Opt Soc Am A* 1999;16:995–1004
61. Marcos S, Burns SA. On the symmetry between eyes of wavefront aberration and cone directionality. *Vision Res* 2000;40:2437–2447
- AU5 62. He JC, Burns SA, Marcos S. Cone photoreceptor directionality from reflectometric and psychophysical measurements. *J Opt Soc Am A* 1999;2363–2369
63. Atchison DA, Joblin A, Smith G. Influence of Stiles-Crawford effect apodization on spatial visual performance. *J Opt Soc Am A* 1998;15(9):2545–2551
64. Rynders MC. The Stiles-Crawford effect and an experimental determination of its impact on vision. Bloomington: Indiana University, 1994
65. Atchison DA, Scott DH, Strang NC, Artal P. Influence of Stiles-Crawford apodization on visual acuity. *J Opt Soc Am A* 2002;19:1073–1083
- AU3 66. Atchison DA, Marcos S, Scott DH. The influence of the Stiles-Crawford peak location on visual performance. *Vision Res* (submitted) 2002
67. Howland HC, Howland B. A subjective method for the measurement of the monochromatic aberrations of the eye. *J Opt Soc Am A* 1977;67:1508–1518
68. Porter J, Guirao A, Cox I, Williams D. Monochromatic aberrations of the human eye in a large population. *J Opt Soc Am A* 2001;18:1793–1803
69. Castejon-Mochon FJ, Lopez-Gil N, Benito A, Artal P. Ocular wave-front aberration statistics in a normal young population. *Vision Res* 2002;42:1611–1617
70. Keller P, Collins M, Carney L, et al. The relation between corneal and total astigmatism. *Optom Vis Sci* 1996;73:86–91
71. Millodot M, Sivak J. Contribution of the cornea and lens to the spherical aberration of the eye. *Vision Res* 1979;19:685–687
72. Artal P, Berrio E, Guirao A, Piers P. Contribution of the cornea and internal surfaces to the change of ocular aberrations with age. *J Opt Soc Am A* 2002;19:137–143
73. Lopez-Gil N, Iglesias I, Artal P. Retinal image quality in the human eye as a function of the accommodation. *Vision Res* 1998;38(19):1–11
74. Atchison D, Collins M, Wildsoet C, et al. Measurement of monochromatic ocular aberrations of human eyes as a function of accommodation by the Howland aberroscope technique. *Vision Res* 1995;35:313–323
75. He JC, Burns SA, Marcos S. Monochromatic aberrations in the accommodated human eye. *Vision Res* 2000;40:41–48
76. Morgan MW. The clinical aspects of accommodation and convergence. *Am J Optom Arch Am Acad Optom* 1944;21:301–313
77. Koretz J, Cook C, Kaufman P. Accommodation and presbyopia in the human eye. Changes in the anterior segment and crystalline lens with focus. *Invest Ophthalmol Vis Sci* 1997;38:569–578

78. Koretz J, Cook C, Kaufman P. Aging of the human lens: changes in lens shape upon accommodation and with accommodative loss. *J Opt Soc Am A* 2002;19:144–151
79. Hofer H, Artal P, Singer B, et al. Dynamics of the eye's wave aberration. *J Opt Soc Am A* 2001;18(3):497–506
80. Artal PFM, Miranda I, Navarro R. Effects of aging in retinal image quality. *J Opt Soc Am A* 1993;10:1656–1662
81. van den Berg T. Analysis of intraocular straylight, especially in relation to age. *Optom Vis Sci* 1995;72:52–59
82. Calver R, Cox M, Elliott D. Effect of aging on the monochromatic aberrations of the human eye. *J Opt Soc Am A* 1999;16:2069–2078
83. McLellan J, Marcos S, Burns S. Age-related changes in monochromatic wave aberrations in the human eye. *Invest Ophthalmol Vis Sci* 2001;1390–1395
84. Artal P, Guirao A. Contributions of the cornea and the lens to the aberrations of the human eye. *Optics Lett* 1998;23(21):1713–1715
85. Glasser A, Campbell M. Presbyopia and the optical changes in the human crystalline lens with age. *Vision Res* 1998;38(2):209–229
86. Jennings JAM, Charman WN. Off-axis image quality in the human eye. *Vision Res* 1981;21:445–455
87. Navarro R, Artal P, Williams DR. Modulation transfer of the human eye as a function of retinal eccentricity. *J Opt Soc Am A* 1993;10(2):201–212
88. Guirao A, Artal P. Off-axis monochromatic aberrations estimated from double pass measurements in the human eye. *Vision Res* 1999;39(2):207–217
89. Navarro R, Moreno E, Dorransoro C. Monochromatic aberrations and point-spread functions of the human eye across the visual field. *J Opt Soc Am A* 1998;15:2522–2529
90. Collins MJ, Wildsoet CF, Atchinson DA. Monochromatic aberrations and myopia. *Vision Res* 1995;35:1157–1163
91. Marcos S, Moreno-Barriuso E, Llorente L, et al. Do myopic eyes suffer from larger amount of aberrations? In: Thorn F, Troilo D, Gwiazda J, eds. *Myopia 200. Proceedings of the Eight International Conference on Myopia*. Boston: International Conference on Myopia, 2000 Press, 2000
- AU6 92. Marcos S, Barbero S, Llorente L. Why high myopic eyes tend to be more aberrated? *Optical Society of America Technical Digest*. Long Beach, CA, 2001
93. Chan D. Bilateral circumscribed posterior keratoconus. *J Am Optom Assoc* 1999;70(9):581–586
94. Schwiegerling J. Cone dimensions in keratoconus using zernike polynomials. *Optom Vis Sci* 1997;74(11):963–969
95. Oshika T, Klyce SD, Applegate RA, et al. Comparison of corneal wavefront aberrations after photorefractive keratectomy and laser in situ keratomileusis. *Am J Ophthalmol* 1999;127:1–127
96. Applegate RA, Howland HC, Sharp RP, et al. Corneal aberrations and visual performance after radial keratotomy. *J Refract Surg* 1998;14:397–407
97. Seiler T, Kaemmerer M, Mierdel P, Krinke H-E. Ocular optical aberrations after photorefractive keratectomy for myopia and myopic astigmatism. *Arch Ophthalmol* 2000;118:17–21
98. Moreno-Barriuso E, Merayo-Llodes J, Marcos S, et al. Ocular aberrations before and after myopic corneal refractive surgery: LASIK-induced changes measured with laser ray tracing. *Invest Ophthalmol Vis Sci* 2001;42:1396–1403
99. Marcos S. Aberrations and visual performance following standard laser vision correction. *J Refract Surg* 2001;17:596–601
100. Marcos S, Barbero B, Llorente L, Merayo-Llodes J. Optical response to LASIK for myopia from total and corneal aberrations. *Invest Ophthalmol Vis Sci* 2001;42:3349–3356
101. Gatinel D, Hoang-Xuan T, Azar D. Determination of corneal asphericity after myopia

surgery with the excimer laser: a mathematical model. *Invest Ophthalmol Vis Sci* 2001;42:1736–1742

102. Norrby N, Grossman L, Geraghty E, et al. Determining the imaging quality of intraocular lenses. *J Cataract Refract Surg* 1998;24:703–714

103. Artal P, Marcos S, Navarro R, et al. Through-focus image quality of eyes implanted with monofocal and multifocal intraocular lenses. *Opt Engine* 1995;34:772–779

104. Guirao A, Redondo M, Geraghty E, et al. Corneal optical aberrations and retinal image quality in patients implanted with monofocal IOLs. *Arch Ophthalmol* (in press) 2002

AU3

105. Barbero S, Marcos S, Llorente L. Optical changes in corneal and internal optics with cataract surgery. *Invest Ophthalmol Vis Sci* (suppl) (in press) 2002;73

AU3